ELSEVIER

Journal of Photochemistry and Photobiology A: Chemistry 133 (2000) 59–66

Journal of Photochemistry and Photobiology A:Chemistry

www.elsevier.nl/locate/jphotochem

Visible light-induced catalytic degradation of iprobenfos fungicide by poly(3-octylthiophene-2,5-diyl) film

C. Wen [a], K. Hasegawa [a,*], T. Kanbara [a], S. Kagaya [a], T. Yamamoto [b]

[a] *Department of Chemical and Biochemical Engineering, Faculty of Engineering, Toyama University, 3190 Gofuku, Toyama 930-8555, Japan*
[b] *Research Laboratory of Resources Utilization, Tokyo Institute of Technology, 4259 Nagatsuta, Midori-ku, Yokohama 226-8503, Japan*

Received 13 September 1999; received in revised form 6 December 1999; accepted 29 December 1999

Abstract

Visible light-induced catalytic degradation of iprobenfos fungicide was investigated using poly(3-octylthiophene-2,5-diyl) (POTh) film by varying oxygen pressure of bubbling gases. The degradation rate increased with the increasing oxygen pressure and obeyed a first-order kinetics in bubbling air. Even after 10 h irradiation (λ>380 nm), the film was substantially stable and no peeling was observed. The quenching of photoluminescence of POTh with O_2 was observed and the formation of active oxygen species such as H_2O_2 and $^{\bullet}OH$ was detected spectrophotometrically. An OH adduct of iprobenfos as well as decomposed intermediates and SO_4^{2-} was also confirmed. The addition of Fe^{2+} accelerated the photocatalytic degradation of iprobenfos by the POTh film. Based on these results, a photocatalytic degradation mechanism is proposed.

Keywords: Polythiophene film; Photocatalytic degradation; Visible light; Active oxygen species; Fungicide

1. Introduction

Water contamination by agrochemicals has received considerable attention because of their toxity, persistence, and widespread utilization. Many agrochemicals have been detected in rivers, lakes, and their sediments [1,2]. Among several wastewater treatments, photocatalytic degradation using TiO_2 is of considerable interest because of its high oxidizing ability [3–5], mineralization [6,7], and use of solar energy [6]. Since TiO_2 is photoexcited by the light of λ<395 nm [3], the development of visible ray-responsive TiO_2 has been performed by addition of metal ions [8–10], metal oxides [11], and photosensitizers [12,13]. The Fenton ($Fe^{2+}+H_2O_2$) and photo-Fenton ($Fe^{2+}/Fe^{3+}+H_2O_2+UV$) processes are another potential techniques for the degradation of water contaminants [14]. To increase the degradation rate using TiO_2, the addition of Fe^{2+} and Fe^{3+} to aqueous TiO_2 suspensions containing phenol has been studied [15].

On the other hand, it has been reported that π-conjugated poly(arylene)s, such as poly(*p*-phenylene), poly(pyridine-2,5-diyl), and poly(2,2′-bipyridine-5,5′-diyl), exhibit photocatalytic reduction of water, ketones, alkenes, and CO_2 in the presence of triethylamine as a sacrificial electron donor [16–18]. Furthermore, a photocatalytic CO_2 fixation reaction on phenol has been studied with poly(3-hexylthiophene-2,5-diyl) film [19]. In contrast to the extensive study for the destruction of water contaminants with TiO_2, only a few investigators have reported the treatment of wastewater using organic materials, such as metallophthalocyanine [20] and polyaniline [21], and much fewer attempts have been made on the photocatalytic process.

As the first application of π-conjugated polymers to the degradation of water pollutants, we have previously reported the results of the photocatalytic degradation of four agrochemicals using poly(3-octylthiophene-2,5-diyl) (POTh) and poly(2,5-dihexoxy-*p*-phenylene) (PHPP) films under bubbling gas and UV light irradiation [22]. Among four agrochemicals, which were specified to monitor by the Environmental Agency of Japan, iprobenfos fungicide decayed rapidly. At the last stage of the irradiation of four agrochemicals, the rate deviated from a first-order kinetics with irradiation time, presumably due to the photodegradation of the films under UV light irradiation [23] and/or peeling of the films in the experimental conditions. Accordingly, counterplans are required for prevention of these defects without pronounced decrease in the efficiency of the decomposition as well as elucidation of the photocatalytic mechanism.

* Corresponding author. Tel.: +81-76-445-6864; fax: +81-76-445-6703.
E-mail address: hasegawa@eng.toyama-u.ac.jp (K. Hasegawa)

1010-6030/00/$ – see front matter
PII: S1010-6030(00)00206-9

Since the POTh film possesses a strong absorption band at λ_{max}=504 nm, it can be activated by visible light. We here report the visible light-induced catalytic degradation of iprobenfos using the POTh film by varying the oxygen pressure of bubbling gases and the acceleration effect of Fe^{2+} on the degradation. Furthermore, we propose the degradation mechanism based on the analyses of the active oxygen species and the decomposed intermediates.

2. Experimental details

2.1. Materials

All reagents were special grade (Wako Pure Chemicals) and used without further purification. POTh was prepared by the oxidative-coupling procedure with $FeCl_3$ as the reported literature [24]. The structures of iprobenfos (IBP) and POTh are shown below.

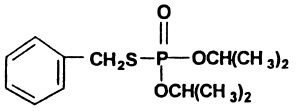

Iprobenfos

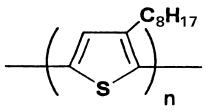

POTh, Mn: 37100

The POTh film was obtained by spin-coating with about 0.2 cm^3 of $CHCl_3$ solution (soluble portion in $CHCl_3$: 45%) containing POTh (15 g dm^{-3}) on a quartz plate (19 mm×38 mm). The POTh film had approximately 10 μm thickness and an absorption maximum at 504 nm with an absorption edge at 670 nm. The POTh coated test tube (18.4 mm i.d. and 50 mm in height of the POTh film) was prepared by painting with 0.3 cm^3 of $CHCl_3$ solution of POTh (3.33 g dm^{-3}) and then evaporating $CHCl_3$.

2.2. Photoreactor

Three types of photoreactor were used in our experiment. The first set of experiment was performed using a WACOM HX-500Q apparatus [25] equipped with a 500 W ultra high-pressure mercury lamp or a 500 W tungsten lamp to examine the photocatalytic function correlated with an absorption property of the POTh film and the effect of oxygen pressure on the photocatalytic degradation. The second experiment was performed using a RH400-10 W apparatus (Riko Co.) equipped with a 400 W high-pressure mercury lamp while circulating a mixed solution composed of 0.25 mol dm^{-3} $NaNO_3$ and 0.10 mol dm^{-3} $NaNO_2$ to examine the addition effect of Fe^{2+} and the decomposed intermediates. The wavelength was selected by a glass filter in combination with a solution filter. A Pyrex filter was used to pass light of λ>290 nm. Visible irradiation of λ>380 nm and λ=435 nm was made with a 500 W ultra high-pressure mercury lamp via a solution filter (0.25 mol dm^{-3} $NaNO_3$+0.10 mol dm^{-3} $NaNO_2$, 1.5 cm thickness) and a Corning 3–73 cut-off filter (λ>420 nm) in combination with a Corning 7–59 band-pass filter (290 nm<λ<500 nm), respectively. UV irradiation of λ=365 nm was obtained with a Toshiba UV-D35 cut-off filter (λ>350 nm) in combination with a Toshiba UV-D36A band-pass filter (300 nm<λ<380 nm). Irradiation of λ>630 nm was performed with a 500 W tungsten lamp via a Toshiba R-69 cut-off filter.

2.3. Procedure

The quartz plate coated with the POTh film was vertically immersed in the reaction cell (light-path length 10 mm×width 20 mm×height 40 mm) containing 5 cm^3 of IBP solution (10 mg dm^{-3}) and gas (N_2, air, or O_2) was bubbled at a flow rate of 50 cm^3 min^{-1} through the solution in the dark for 30 min at 30°C. After IBP was reached to the adsorption equilibrium between the POTh film and the solution, the cell was irradiated with light of λ>290, λ>380, λ=435, λ=365 nm or λ>630 nm. Direct photolysis was performed under the same reaction conditions except for using the POTh film. The quantity of light (I_0) entered the reaction cell was measured with potassium tris (oxalato) ferrate (III) actinometry and corrected for the quantum yields of Fe^{2+} formation. I_0 was estimated as follows (photons cm^{-2} s^{-1}): λ>290 nm, $I_0=8.1\times10^{16}$ for 290–500 nm; λ>380 nm, $I_0=4.2\times10^{16}$ for 380–500 nm; λ=435 nm, $I_0=0.62\times10^{16}$, and λ×365 nm, 1.3×10^{16}.

For investigating the addition effect of Fe^{2+} on the degradation, different amounts of $FeCl_2$ was added to 10 cm^3 IBP solution (10 mg dm^{-3}) in the POTh coated test tube, which was irradiated at λ>380 nm for 10 h at air flow rate of 50 cm^3 min^{-1}. I_0 entered the IBP solution (10 cm^3) was also corrected for the quantum yields of Fe^{2+} formation and was estimated to be 1.5×10^{17} photons s^{-1} for 380–500 nm. To collect the decomposed intermediates, the test tube containing 20 cm^3 of IBP solution (20 mg dm^{-3}) was irradiated for 20 h and the solution was loaded into a Waters Sep-Pak cartridge and the adsorbed intermediates were eluted with CH_3CN. This step is called as solid phase extraction method (SPE). The solution was concentrated to 0.1 cm^3 under N_2 purge for GC and GC-MS measurements.

Experiments for the determination of H_2O_2 and detection of $^{\bullet}OH$ were made in the reaction cell immersed with POTh film-coated quartz plate at λ>380 nm. pH was adjusted by addition of aqueous H_2SO_4 or NaOH.

2.4. Analysis

About 30 μl of the irradiated solution was withdrawn in certain intervals and the concentration of IBP was measured by a JASCO HPLC system equipped with a PU-980 pump, an 870 UV–VIS detector, a Cica-Merck Lichrospher 100 RP-18 column (10 cm long, 4.6 mm i.d.). A mixture

of CH_3CN: H_2O=65:35 was used as a mobile phase. The structures of the decomposed intermediates were examined with a GC-MS (JEOL 700Q) equipped with a fused silica capillary column (HP-5, 30 m long, 0.32 mm i.d.).

Fluorescence spectrum of POTh in $CHCl_3$ (1.2 mg dm^{-3}) was measured at λ_{ex}=470 nm after a $CHCl_3$ solution was separately bubbled with N_2, air, a mixture of N_2 and O_2, and O_2, and it was also measured by varying the concentration of IBP (2, 5 and 10 mg dm^{-3}) under N_2. IR and UV–VIS spectra of the POTh film were recorded with a JASCO FT/IR 230 and a Shimadzu UV-1600 spectrometers, respectively. Inorganic ions were measured by a Dionex 2000i ion chromatograph equipped with a Tosoh IC-anion-PW anion column using a mixed solution of 1.0 mmol dm^{-3} Na_2CO_3 and 0.375 mmol dm^{-3} $NaHCO_3$ as an eluent.

H_2O_2 and $^{\bullet}OH$ formed in the photoirradiated solution were determined and detected by the titanium method [26] and the thiobarbituric acid (TBA) method [27,28], respectively. To determine the concentration of H_2O_2 generated in aqueous solutions of various pH, 5 cm^3 of each aqueous solution was irradiated in the presence of the POTh film for 30 min under bubbling air and then a Ti-H_2SO_4 reagent (2.5 cm^3) and a 1:1 H_2SO_4 (6.25 cm^3) were added. After being warmed at 60°C for 10 min, the absorbance of the solution was measured at 407 nm. To detect $^{\bullet}OH$, 5 cm^3 of the aqueous solution containing deoxyribose (2.8×10^{-5} mol dm^{-3}) and various amounts of $FeCl_2$ was irradiated at 37°C for 120 min under bubbling air and 1.2 cm^3 of the solution was then transferred into a test tube, which contained 1% TBA solution (1 cm^3) and 2.8% HCl (1 cm^3). After being warmed at 100°C for 60 min, the absorbance of the solution was measured.

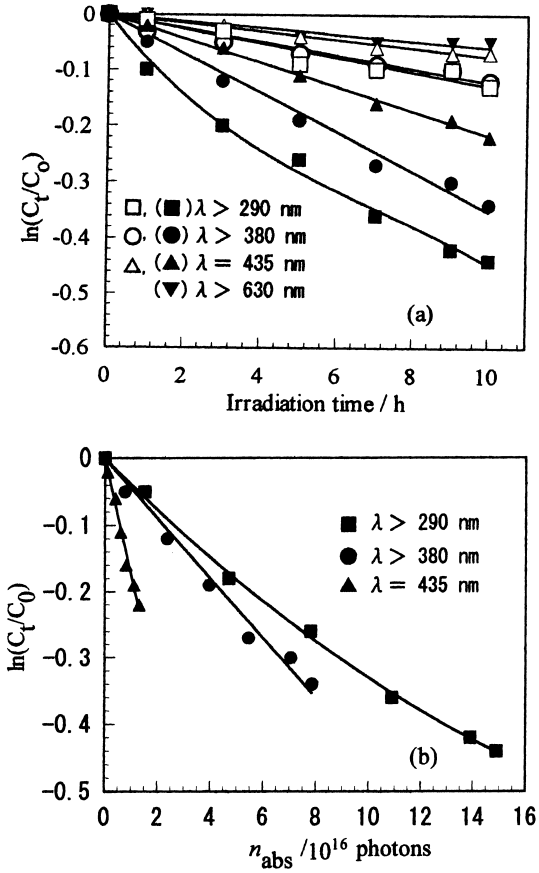

Fig. 1. Effects of irradiation wavelength on the degradation of IBP with and without the POTh film under bubbling air. With POTh film (■, ●, ▲ and ▼), without POTh film (□,○ and △). (a) Degradation of IBP versus time; (b) degradation of IBP versus photons. $[IBP]_0$=10 mg dm^{-3}.

3. Results and discussion

3.1. Visible light-induced catalytic degradation of IBP

Fig. 1a shows the effect of irradiation wavelength on the degradation of IBP with and without the POTh film under bubbling air. When the POTh film was used, irradiation with light of 290 nm<λ<630 nm caused the degradation of IBP, whereas irradiation with light of λ>630 nm hardly caused the degradation. These results show that the photoexcited film causes the photocatalytic degradation of IBP since the film exhibits an absorption band based on π-π* transition in the range of 290–670 nm (λ_{max}=504 nm). It is very interesting that the photocatalytic degradation of IBP is induced by visible light irradiation (λ>380 nm) owing to effective utilization of solar energy.

Fig. 1b displays the degradation of IBP versus the photon numbers entered the reaction cell. The degradation rate increases in the order λ=435 nm>λ>380 nm>λ>290 nm, which is correlated with an absorption property of the POTh film. Furthermore, the quantum yield of $\Phi_{435\,nm}$ (3.8×10^{-4}) was larger than $\Phi_{365\,nm}$ (1.8×10^{-4}). These results suggest that the film is operative in the range of visible light irradiation for the degradation of IBP.

As described in the previous paper [22], under light irradiation of λ>290 nm, the degradation rate deviated from a first-order kinetics with irradiation time due to partial photodegradation of the film under UV light irradiation and/or peeling of the film in the experimental conditions. Caronna et al. [23] reported that visible light caused the photodegradation of poly(3-butylthiophene) film to yield two low molecular weight products. On the contrary, Kawai et al. [29] reported that once *m*-ter-butylphenol was added, poly(3-hexylthiophene) film showed no degradation after the photocatalytic CO_2 fixation to the phenol. In the present study, no detectable degradation and peeling of the POTh film were observed even after 10 h irradiation (λ>380 nm and λ=435 nm) under bubbling air. The stability of the film was confirmed by IR and UV–VIS spectrometry. Although the deterioration mechanism of the film by UV light irradiation was not examined, it may proceed through oxidation of the polymeric chains by singlet oxygen as suggested by Caronna et al. [23].

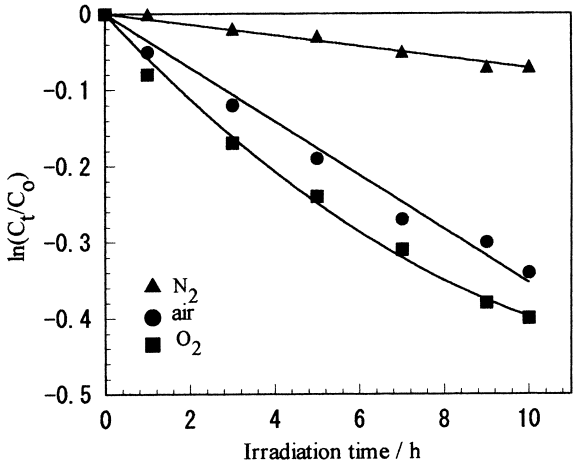

Fig. 2. Effect of bubbling gas on the photocatalytic degradation of IBP by the POTh film under visible light irradiation. λ>380 nm, $[IBP]_0$=10 mg dm^{-3}.

3.2. Effect of oxygen pressure on the photocatalytic degradation

Fig. 2 shows the effect of bubbling gas on the photocatalytic degradation of IBP with the POTh film under visible light irradiation (λ>380 nm). Under bubbling N_2, the degradation rate of IBP is very slow, while it is obviously increased under bubbling air and O_2. The rate increases in the following order O_2>air>N_2. This fact indicates that the increase in the oxygen pressure promotes the degradation of IBP.

3.3. Detection of active oxygen species

Since the photocatalytic degradation increased with the increasing oxygen pressure, the formation of active oxygen species in the irradiated solution was examined. Fig. 3 shows Stern–Volmer plots of fluorescence quenching of POTh by O_2 in $CHCl_3$. Relative fluorescence intensity (I_0/I) increases linearly with increasing oxygen pressure as shown in Eq. (1).

$$\frac{I_0}{I} = 1 + k_q P_{O_2} \quad (1)$$

From the slope of the Stern–Volmer plots, the fluorescence quenching constant (k_q) is estimated to be 3.6×10^{-3} kPa^{-1}. The value of k_q seems to be related to the formation of $O_2^{\bullet-}$ by electron transfer from excited POTh to molecular oxygen. The fluorescence quenching of POTh by IBP in $CHCl_3$ was not observed under N_2. This result shows that electron transfer from excited POTh to IBP can not proceed. The fluorescence quenching of poly(3-hexylthiophene) film with CO_2 [29] and poly(*p*-terphenyl) with O_2 [30] has been reported.

The formation of $O_2^{\bullet-}$ encouraged us to consider that the photocatalytic process using the POTh film involves a series of active oxygen species, such as $O_2^{\bullet-}$, $HO_2^{\bullet}$, H_2O_2 and $^{\bullet}$OH, which have been found when TiO_2 was used as a photocatalyst [3]. As expected, ca. 0.09 and 0.07 μmol H_2O_2 were determined by the titanium method [26] after visible light irradiation (λ>380 nm) for 30 and 60 min, respectively. This result indicates that H_2O_2 can be produced on the surface of the POTh film. Fig. 4 demonstrates the effect of pH on the yield of H_2O_2. The production of H_2O_2 decreases with increasing pH of the aqueous solution and diminishes to zero at pH>10. This pH dependence of H_2O_2 formation corresponds with the result reported by Fujihira et al. for TiO_2 suspended aqueous solution [31].

The formation of $^{\bullet}$OH in the presence of the POTh film was indirectly identified by the TBA method [27,28]. Fig. 5 shows absorption spectra of the aqueous solution obtained from the TBA reaction. The absorption peak in the neighborhood of 500 nm is characteristic of the pigment. An absorption at λ=500 nm was apparently observed in the presence of Fe^{2+} (spectrum a), whereas the absorption at λ=503 nm is low in the absence of Fe^{2+} (spectrum b). This result suggests that $^{\bullet}$OH can be produced under visible light irradiation (λ>380 nm) by the decomposition of H_2O_2 formed during the photocatalytic process although

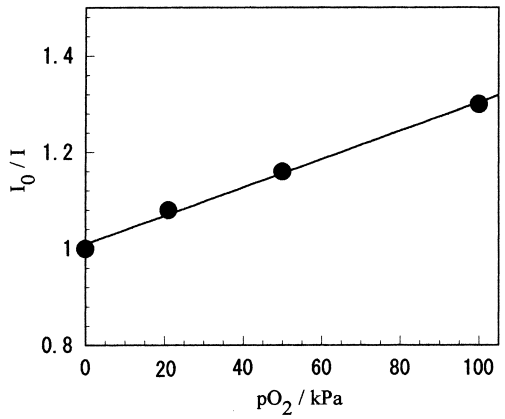

Fig. 3. Stern–Volmer plots of fluorescence of POTh in $CHCl_3$. $[POTh]_0$=1.2 mg dm^{-3}, λ_{ex}=470 nm, λ_{em}=570 nm.

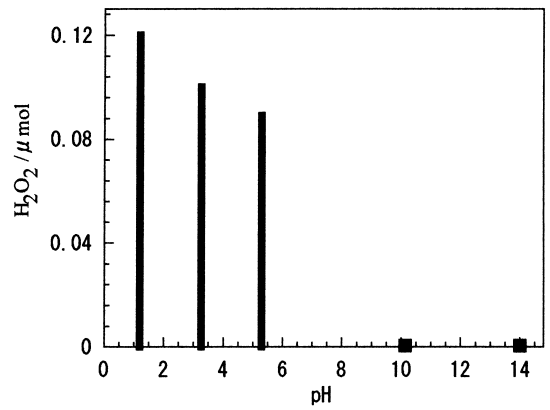

Fig. 4. Effect of pH on the formation of H_2O_2 by the POTh film in aqueous solution under visible light irradiation (λ>380 nm) for 30 min.

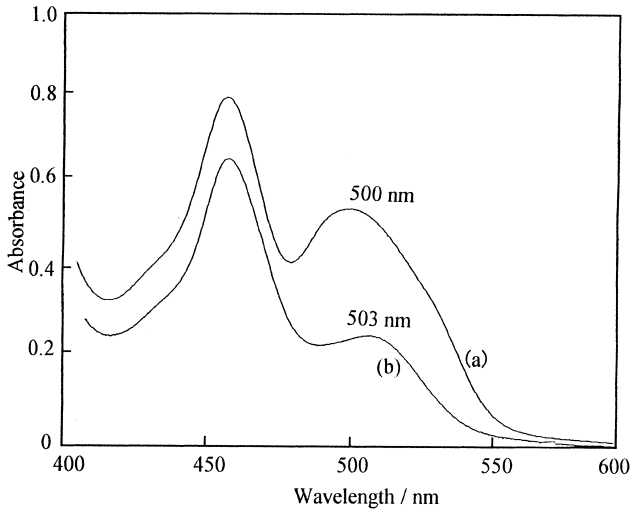

Fig. 5. Absorption spectra of the pigment formed by the TBA method using the POTh film under visible light irradiation (λ>380 nm). (a) In the presence of Fe^{2+}(5×10^{-4} mol dm^{-3}); (b) in the absence of Fe^{2+}.

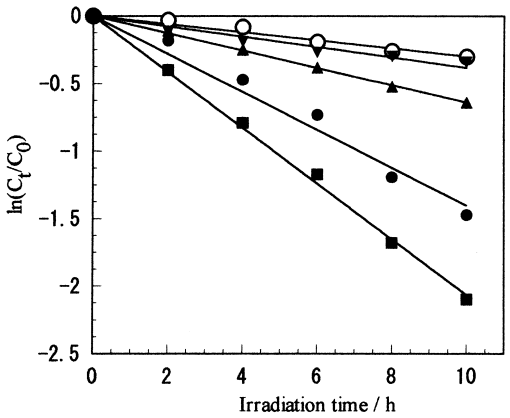

Fig. 6. Effect of Fe^{2+} concentration on the degradation of IBP with the POTh film (■, ●, ▲, ▼) and without the POTh film (○) under visible light irradiation (λ>380 nm). (○) $[Fe^{2+}]_0=5\times10^{-4}$ mol dm^{-3}; (▼) $[Fe^{2+}]_0=0$; (▲) $[Fe^{2+}]_0=5\times10^{-3}$ mol dm^{-3}; (■) $[Fe^{2+}]_0=5\times10^{-4}$ mol dm^{-3}; (●) $[Fe^{2+}]_0=5\times10^{-5}$ mol dm^{-3}; $[IBP]_0=10$ mg dm^{-3}.

the amount of $^{\bullet}OH$ is less than that in the presence of Fe^{2+}. Direct photolysis of H_2O_2 produces $^{\bullet}OH$, however, because H_2O_2 weakly absorbs solar radiation, $^{\bullet}OH$ formation by this method is comparatively slow [32].

Based on these experimental results, the mechanism of the acceleration effect of Fe^{2+} on the photocatalytic degradation is similar to the photo-Fenton reaction. The mechanism can be explained based on the Eqs. (2)–(4), in which conversion of Fe^{2+} to Fe^{3+} leads to increased amounts of H_2O_2 and $^{\bullet}OH$ [33–35].

$$Fe^{2+} + O_2^{\bullet-} + 2H^+ \rightarrow Fe^{3+} + H_2O_2 \quad (2)$$

$$Fe^{2+} + HO_2^{\bullet} + H^+ \rightarrow Fe^{3+} + H_2O_2 \quad (3)$$

$$Fe^{2+} + H_2O_2 + H^+ \rightarrow Fe^{3+} + {}^{\bullet}OH + H_2O \quad (4)$$

3.4. Acceleration effect of Fe^{2+} on the photocatalytic degradation

Based on the observation shown in Fig. 5, we further investigated the effect of Fe^{2+} addition on the photocatalytic degradation of IBP. As shown in Fig. 6, the addition of Fe^{2+} accelerated the degradation and the maximum photoreactivity was observed at $[Fe^{2+}]=5\times10^{-4}$ mol dm^{-3}. Similar effects of Fe^{2+} addition have been reported for the photocatalytic degradation of phenol in aqueous TiO_2 dispersions in the presence of Fe^{3+} and Fe^{2+} [15]. At $[Fe^{2+}]=5\times10^{-4}$ mol dm^{-3}, the degradation rate of IBP was 2.5 times than that in the absence of Fe^{2+}, indicating that the photo-Fenton reaction was exerted most efficiently. Therefore, the decomposition of H_2O_2 is an important kinetic step in the photocatalytic degradation of IBP.

3.5. Photocatalytic degradation intermediates and pathways

After ca. 96% of IBP was decomposed photocatalytically under the optimum concentration of Fe^{2+} (5×10^{-4} mol dm^{-3}), the intermediates were analyzed by using GC and GC-MS methods. All GC peak areas assignable to the intermediates are 6.4 times that of residual IBP, that is, corresponding to 26% of the peak area of IBP before irradiation. This fact shows that ca. 74% of IBP decomposed to water-soluble small molecules/ions and they were not extracted by the SPE method. In fact, mineralized SO_4^{2-} was detected in the aqueous filtrate with ion chromatography.

Fig. 7 shows a total ion chromatogram (TIC) of decomposed intermediates. The structures of the intermediates identified/estimated are shown on the top of the peaks and the peak numbers designate them. The structures of 1, 2, 3, 6 and 13 were identified by comparing the mass spectra and GC retention times with those of the standard samples. The structures of 4, 5, 7, 8, 9, 10, 11, 12 and 14 were estimated from the molecular ion mass and fragment patterns because a number of their isomers were not available. The structures of the others were hitherto obscure. Table 1 lists their characteristic ions mass and their assignment. We have previously reported the photocatalytic degradation of IBP using TiO_2 particles and proposed the degradation pathways based on the intermediate analysis [25]. Both the intermediates obtained by using the POTh film and TiO_2 particles were similar.

Based on the product analyses, degradation pathways of IBP are proposed in Scheme 1. One pathway is the C–S bond attack of IBP by $^{\bullet}OH$ to give 3, 6 and 9. Second pathway is the OH attack on the C–S bond accompanying with the benzene ring attack of isopropyl radicals to afford 7, 10, 11 and 12. The isopropyl radical may be produced by the C–O bond cleavage as observed in the photocatalytic degradation

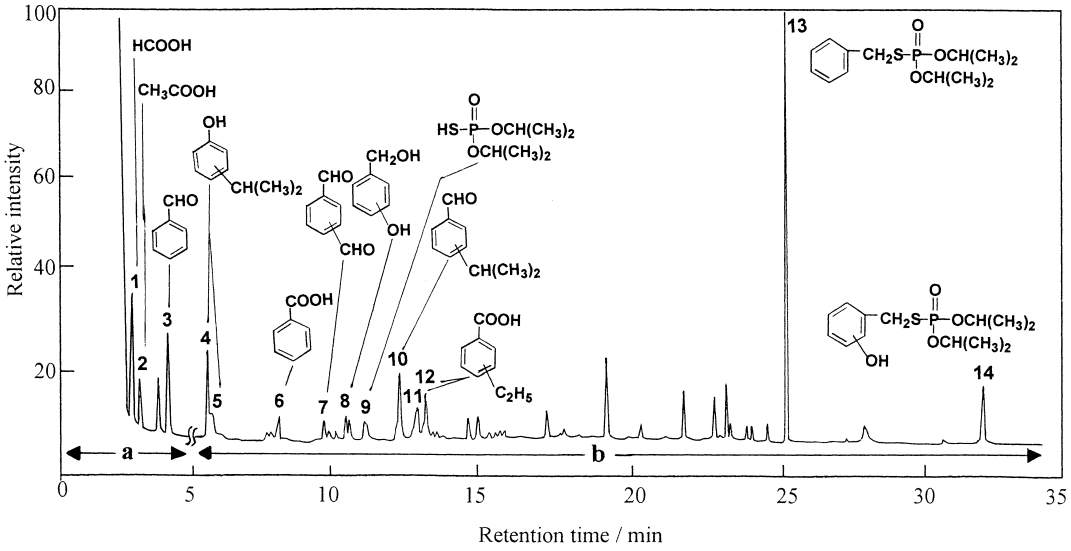

Fig. 7. Total ion chromatogram of the decomposed intermediates of IBP. GC-MS condition: (a) 50°C; (b) 70°C→5°C min^{-1}→270°C.

Table 1
Characteristic ion mass of the degradation intermediates of IBP

Peak No.	Characteristic ion mass (*m/z*) and assignment
1	46 (M^+), 45 (M^+-H), 29 (HCO^+), 17 (OH^+)
2	60 (M^+), 45 (M^+-CH_3), 43 (CH_3CO^+)
3	106 (M^+), 77 (M^+-CHO), 51 ($M^+-CHO-C_2H_2$)
4, 5	136 (M^+), 121 (M^+-CH_3), 104 (M^+-CH_3-OH), 91 ($C_6H_5CH_2^+$), 77 ($C_6H_5^+$)
6	122 (M^+), 105 (M^+-OH), 94 (M^+-CO), 91 ($C_6H_5CH_2^+$), 77 ($M^+C_6H_5^+$)
7	134(M^+), 133 (M^+-H), 105 (M^+-CHO), 77 ($C_6H_5^+$)
8	124 (M^+), 106 (M^+-H_2O), 78 ($C_6H_6^+$)
9	198 (M^+), 156($M^+-C_3H_6$), 141($M^+-OC_3H_7+2H$), 114 ($M^+-2C_3H_6$), 59 ($C_3H_7O^+$)
10	148(M^+), 133 (M^+-CH_3), 119 (M^+-CHO), 105 ($M^+-CH(CH_3)_2$), 91 ($C_6H_5CH_2^+$), 77 ($C_6H_5^+$)
11, 12	150(M^+), 135 (M^+-CH_3), 105 (M^+-CO_2H), 91 ($C_6H_5CH_2^+$), 77 ($C_6H_5^+$)
13	288(M^+), 246 ($M^+-C_3H_6$), 204 ($M^+-2C_3H_6$), 123 ($C_6H_5CH_2S^+$), 91 ($C_6H_4CH_2^+$), 77 ($C_6H_5^+$)
14	304(M^+), 262 ($M^+-C_3H_6$), 220 ($M^+-2C_3H_6$), 139 ($C_6H_4(OH)CH_2S^+$), 107 ($C_6H_4(OH)CH_2^+$), 77 ($C_6H_5^+$)

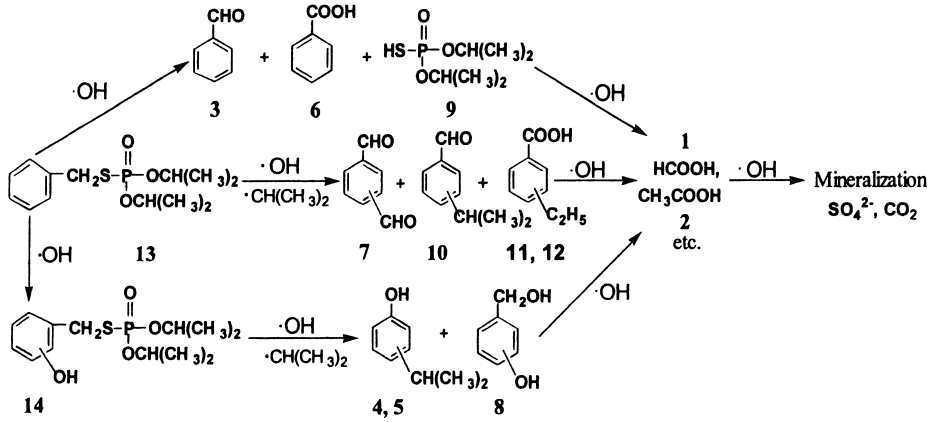

Scheme 1. Degradation pathways.

of IBP using TiO_2 [25]. Third pathway is addition of OH to the benzene ring of IBP, followed by the C–S or the C–C bond attack of $^{\bullet}OH$ accompanying with the benzene ring attack of isopropyl radicals to yield 4, 5 and 8. All the intermediates are ultimately mineralized to give SO_4^{2-} and CO_2 via volatile organic acids such as HCOOH and CH_3COOH.

3.6. Postulated photocatalytic processes

Considering the formations of the OH adduct of IBP and active oxygen species such as $O_2^{\bullet-}$, H_2O_2 and $^{\bullet}OH$, a possible photocatalytic process of the POTh film is suggested in Eqs. (5)–(15).

(a) Generation of superoxide

$$\mathrm{POTh} + h\nu(\lambda > 380\,\mathrm{nm}) \rightarrow \mathrm{POTh}^* \quad (5)$$

$$\mathrm{POTh}^* + \mathrm{O_2} \rightarrow \mathrm{POTh}^{\bullet+} + \mathrm{O_2}^{\bullet-} \quad (6)$$

(b) Generation of hydrogen peroxide

$$\mathrm{O_2}^{\bullet-} + \mathrm{H}^+ \rightarrow \mathrm{HO_2}^{\bullet} \quad (7)$$

$$\mathrm{O_2}^{\bullet-} + \mathrm{HO_2}^{\bullet} + \mathrm{H}^+ \rightarrow \mathrm{H_2O_2} + \mathrm{O_2} \quad (8)$$

$$\mathrm{HO_2}^{\bullet} + \mathrm{H}^+ + \mathrm{e}^-(\mathrm{POTh}^*) \rightarrow \mathrm{H_2O_2} \quad (9)$$

$$\mathrm{HO_2}^{\bullet} + \mathrm{HO_2}^{\bullet} \rightarrow \mathrm{H_2O_2} + \mathrm{O_2} \quad (10)$$

(c) Generation of hydroxyl radical

$$\mathrm{H_2O_2} + h\nu(\lambda > 380\,\mathrm{nm}) \rightarrow 2^{\bullet}\mathrm{OH} \quad (11)$$

$$\mathrm{H_2O_2} + \mathrm{O_2}^{\bullet-} \rightarrow {}^{\bullet}\mathrm{OH} + \mathrm{OH}^- + \mathrm{O_2} \quad (12)$$

$$\mathrm{H_2O_2} + \mathrm{e}^-(\mathrm{POTh}^*) \rightarrow {}^{\bullet}\mathrm{OH} + \mathrm{OH}^- \quad (13)$$

(d) Regeneration of POTh

$$4\mathrm{POTh}^{\bullet+} + 2\mathrm{H_2O} \rightarrow 4\mathrm{POTh} + \mathrm{O_2} + 4\mathrm{H}^+ \quad (14)$$

$$\mathrm{POTh}^{\bullet+} + \mathrm{IBP} \rightarrow \mathrm{POTh} + \mathrm{IBP}^{\bullet+} \quad (15)$$

The POTh film can be photoexcited under visible irradiation (Eq. (5)). When O_2 is present as a quencher in the photocatalytic reaction, $POTh^*$ is quenched to give $O_2^{\bullet-}$ and $POTh^{\bullet+}$ (Eq. (6)). Since $O_2^{\bullet-}$ is an unstable weak base (pKa=4.88) in an aqueous solution and is known to exist in equilibrium with H^+ (Eq. (7)) [36], the formation of $HO_2^{\bullet}$ would be accelerated by addition of acid. Therefore, the promotion of H_2O_2 at lower pH (Fig. 4) is reasonably explained by Eqs. (7)–(10) [37]. The generation of $^{\bullet}OH$ (Fig. 5) may be explained by the photocatalytic decomposition of H_2O_2 (Eq. (11)), and H_2O_2 also may be reduced by $O_2^{\bullet-}$ or excited electrons to generate $^{\bullet}OH$ (Eqs. (12) and (13)) [38,39]. The $^{\bullet}OH$ may not be formed from direct oxidation of OH^- because the oxidation potential (E_{ox}) of OH^- (2.0 V versus NHE) is larger than that of the POTh film (ca. 1.3 V versus NHE) [22]. The $POTh^{\bullet+}$ formed via Eq. (6) seems to be reduced by H_2O (Eq. (14)) or IBP (Eq. (15)) to regenerate POTh.

Yanagida et al. [40] studied the photooxidation of benzene in a CH_3CN-H_2O solution of perfluorinated oligo(*p*-phenylene)s (F-OPP-*n*) and proposed that the formation of phenol proceeded through the reaction of benzene with $^{\bullet}OH$ formed by the oxidation of OH^- by F-OPP-$n^{\bullet+}$ in the valence band. Compared with the photooxidation using F-OPP-*n*, the photocatalytic degradation of IBP using the POTh film can be explained to proceed through the oxidation by the $^{\bullet}OH$ formed in the conduction band.

4. Conclusions

The POTh film showed the photocatalytic activity under visible light irradiation without damage of the film and affords photodegradation products of IBP. An addition of Fe^{2+} accelerated the photocatalytic degradation of IBP, which would be mainly related to the actual action of the photo-Fenton reaction. The photocatalytic processes were suggested based on the detection of active oxygen species such as $O_2^{\bullet-}$, H_2O_2 and $^{\bullet}OH$, and an OH adduct of IBP.

POTh has some merits such as good film processability and visible light availability comparing with TiO_2, which is photoexcited by UV light. To compare the photocatalytic activity of POTh and TiO_2, experiments must be made using the same reaction system. Since the quantum yield of IBP degradation using TiO_2 film has not been reported, the quantum yield using the POTh film was compared with that using TiO_2 particles in aqueous suspensions. The photocatalytic activity of the POTh film was inferior to that of TiO_2 particles (POTh film: $\Phi_{365\,nm}=1.8\times10^{-4}$, TiO_2 particles: $\Phi_{365\,nm}=1.2\times10^{-2}$ [25]). The application of TiO_2 particles to the degradation of wastewater treatments is known to be difficult because of their difficult filtration and settling. Although many attempts using TiO_2 film have been made to eliminate the need for these operations, to date this works have largely been unsuccessful [41]. The low activity of the POTh film may be mainly ascribed to the low redox potential compared with that of TiO_2 as well as the low surface area. More progress on the photocatalytic activity of the polymer film is necessary to the treatment of water pollutants.

Acknowledgements

The authors are grateful for the financial support by a grant-in-aid for Scientific Research (No. 10680538) from the Ministry of Education, Science, Sports and Culture of Japan. The authors also wish to thank Miss M. Shinoda for the GC-MS measurement. C. Wen thanks Mr. H. Tsuchikawa for his valuable suggestion on the photo-Fenton reaction and Mr. H. Wang for his useful comments related to analytic method.

References

[1] W.E. Pereira, C.E. Rostad, Environ. Sci. Technol. 24 (1990) 1400.
[2] E.M. Thurman, M.T. Meyer, M.S. Mills, L.R. Zimmerman, C.A. Perry, Environ. Sci. Technol. 28 (1994) 2267.
[3] M.R. Hoffmann, S.T. Martin, W. Choi, D.W. Bahnemann, Chem. Rev. 95 (1995) 69.
[4] T. Hisanaga, K. Harada, K. Tanaka, J. Photochem. Photobiol. A: Chem. 54 (1990) 113.
[5] K. Hofstadler, R. Bauer, S. Novalic, G. Heisler, Environ. Sci. Technol. 28 (1994) 670.
[6] D.F. Ollis, E. Pelizzetti, N. Serpone, Environ. Sci. Technol. 25 (1991) 1523.
[7] G. Mills, M.R. Hoffmann, Environ. Sci. Technol. 27 (1993) 1681.
[8] E. Borgarello, J. Kiwi, M. Gratzel, E. Pelizzetti, M. Visca, J. Am. Chem. Soc. 104 (1982) 2996.
[9] Y. Sakata, Y. Hirata, K. Miyahara, H. Imamura, S. Tsuchiya, Chem. Lett., 1993, 391.
[10] Y. Sakata, T. Yamamoto, T. Okazaki, H. Imamura, S. Tsuchiya, Chem. Lett., 1998, 1253.
[11] Y. Sakata, T. Yamamoto, H. Gunji, H. Imamura, S. Tsuchiya, Chem. Lett., 1998, 131.
[12] K. Sayama, M. Sugino, H. Sugihara, Y. Abe, H. Arakawa, Chem. Lett., 1998, 753.
[13] H. Sugihara, L.P. Singh, K. Sayama, H. Arakawa, Md. K. Nazeeruddin, M. Graetzel, Chem. Lett., 1998, 1005.
[14] M.M. Schere, J.C. Westall, M. Ziomek-Moroz, P.G. Tratnyek, Environ. Sci. Technol. 31 (1997) 2385.
[15] A. Sclafani, L. Palmisano, E. Davi, J. Photochem. Photobiol. A: Chem. 56 (1991) 113.
[16] T. Shibata, A. Kabumoto, T. Shiragami, O. Ishitani, C. Pac, S. Yanagida, J. Phys. Chem. 94 (1990) 2068.
[17] S. Matsuoka, T. Kohzuki, A. Nakamura, C. Pac, S. Yanagida, J. Chem. Soc. Chem. Commun., 1991, 580.
[18] T. Yamamoto, Y. Yoneda, T. Maruyama, J. Chem. Soc. Chem. Commun., 1992, 1652.
[19] T. Kawai, T. Kuwabara, K. Yoshino, J. Chem. Soc. Faraday Trans. 88 (1992) 2041.
[20] T. Ichinohe, A. Isoda, M. Kimura, K. Hanabusa, H. Shirai, Polym. Prepr. Japan 46 (1977) 377.
[21] P. Peralta-zamora, S.G. Moraes, J. Reyes, N. Duran, Polym. Bull. 37 (1996) 531.
[22] K. Hasegawa, C. Wen, T. Kotani, T. Kanbara, S. Kagaya, T. Yamamoto, J. Mater. Soc. Lett. 18 (1999) 1091.
[23] T. Caronna, M. Forte, M. Catellani, S.V. Meille, Chem. Mater. 9 (1997) 991.
[24] R.M.S. Maior, K. Hinkelmann, H. Eckert, F. Wudl, Macromolecules 23 (1990) 1268.
[25] K. Hasegawa, T. Kanbara, S. Kagaya, Denki Kagaku 66 (1998) 625.
[26] H. Pobiner, Anal. Chem. 33 (1961) 1423.
[27] J.M.C. Gutteridge, T.R. Ticken, Anal. Biochem. 91 (1978) 250.
[28] T. Ozawa, H. Goto, F. Takazawa, A. Hanaki, Nippon Kagaku Kaishi. 4 (1988) 459.
[29] T. Kawai, T. Kuwabara, K. Yoshino, Synth. Met. 55/57 (1993) 3649.
[30] T. Kitamura, Y. Wada, K. Murakoshi, M. Kusaba, N. Nakashima, A. Ishida, T. Majima, S. Takamuku, T. Akano, S. Yanagida, J. Chem. Soc. Faraday Trans. 92 (1996) 3491.
[31] M. Fujihira, Y. Satoh, T. Osa, Bull. Chem. Soc. Japan 55 (1982) 666.
[32] R.G. Zepp, B.C. Faust, J. Hoigne, Environ. Sci. Technol. 26 (1992) 313.
[33] K. Wu, T. Zhang, J. Zhao, H. Hidaka, Chem. Lett., 1998, 857.
[34] A.M. Mckinzi, T.J. Dichristina, Environ. Sci. Technol. 33 (1999) 1886.
[35] J.J. Pignatello, D. Liu, P. Huston, Environ. Sci. Technol. 33 (1999) 1832.
[36] K. Okamoto, Y. Yamamoto, H. Tanaka, M. Tanaka, A. Itaya, Bull. Chem. Soc. Japan 58 (1985) 2015.
[37] I. Izumi, F.F. Fan, A.J. Bard, J. Phys. Chem. 85 (1981) 218.
[38] M. Fujihira, Y. Satoh, T. Osa, Nature 293 (1981) 206.
[39] S. Teratani, Y. Takagi, M. Takahashi, H. Noda, A. Ikuo, K. Tanaka, Nippon Kagaku Kaishi 1984, 283.
[40] K. Maruo, Y. Wada, S. Yanagida, Bull. Chem. Soc. Japan 65 (1992) 3439.
[41] A. Mills, R.H. Davies, D. Worsley, Chem. Soc. Rev., 1993, 417.